Extraction, Purification, and Characterization of Microbial Melanin Pigments

Vishal A. Ghadge, Sanju Singh, Pankaj Kumar, Doniya Elze Mathew, Asmita Dhimmar, Harshal Sahastrabudhe, Apexa Gajjar, Satish B. Nimse, and Pramod B. Shinde

1 Introduction

'Melanins' are natural polymeric pigments present in all forms of life, having a heterogeneous origin with an extensive diversity extending from structure, and functions to different colored pigments (Gosset 2017; Stepien et al. 2013). The melanin word was derived from 'melanos' meaning dark. However, a Swedish scientist proved the appearance of melanin in the 1840s after isolating the pigment from the iris of the eye. The initial procedure for the formation of polymeric pigments is via the oxidation of phenolic or indolic monomeric substrates involving enzyme catalysis. Melanin has slowly diversified from three different types into five different classes based on the monomeric unit involved in their formation. Those five types are eumelanin, pheomelanin, allomelanin, pyomelanin, and neuromelanin. Eumelanin and allomelanin contribute dark brown to black coloration to the cells

V. A. Ghadge · S. Singh · P. Kumar · A. Dhimmar · H. Sahastrabudhe · A. Gajjar · P. B. Shinde (✉)
Natural Products & Green Chemistry Division, CSIR-Central Salt and Marine Chemicals Research Institute (CSIR-CSMCRI), Council of Scientific and Industrial Research (CSIR), Bhavnagar, Gujarat, India

Academy of Scientific and Innovative Research (AcSIR), Ghaziabad, Uttar Pradesh, India
e-mail: pramodshinde@csmcri.res.in

D. E. Mathew
Academy of Scientific and Innovative Research (AcSIR), Ghaziabad, Uttar Pradesh, India

Applied Phycology and Biotechnology Division, CSIR-Central Salt and Marine Chemicals Research Institute (CSIR-CSMCRI), Council of Scientific and Industrial Research (CSIR), Bhavnagar, Gujarat, India

S. B. Nimse
Institute of Applied Chemistry and Department of Chemistry, Hallym University, Chuncheon, Republic of Korea

G. Gosset (ed.), *Melanins: Functions, Biotechnological Production, and Applications*, https://doi.org/10.1007/978-3-031-27799-3_5

unbiased for any specific kingdom. Whereas pheomelanin is mainly found in the animal kingdom and provides yellow to red pigmentation to the cells (Nicolaus 1968; Pralea et al. 2019). The precursor units of these melanins play an important role in understanding the synthesis, structure, and function of these pigments. Precursor units for the polymer eumelanin consist primarily of indole-type monomeric units that are formed as a result of L-tyrosine or L-DOPA (L-3,4-dihydroxyphenylalanine) oxidation reactions. Similarly, pheomelanins are also the products of tyrosine as eumelanins, however, cysteine moieties are incorporated in their structures (Singh et al. 2021). The synthesis of allomelanins is quite different and is derived by the oxidation of nitrogen-free diphenols such as catechol, 1,8-dihydroxynaphtalene, and γ-glutaminyl-3,4-dihydroxybenzene. Pyomelanins are polymers of 2,5-dihydroxyphenylacetic acid, a byproduct of tyrosine metabolism, and display better photo- and thermo-stability. Whereas neuromelanin is synthesized from catechol and quinones in the human substantia nigra (Haining and Achat-Mendes 2017; Pralea et al. 2019). Knowledge of the structure and biosynthetic pathways that lead to the various melanins found in nature can act as inspiration for the development of new artificial pigments and their materials. Melanins are well-known for providing pigmentation to cells, however, they play many major roles in different niches of life. Melanins provide shielding from harmful radiations, perform oxidation of reactive oxygen species, are responsible for a range of functions across kingdoms, help with defense mechanisms in arthropods, molluscs, and microbes, and enhance pathogenicity in various fungi and bacteria (Singh et al. 2021). Further, due to the intramolecular electronic interactions, melanins have applications in semiconductors (Bothma et al. 2008), as metal chelators, as optical imagers (Abbas et al. 2009), extending to cosmeceuticals and pharmaceuticals, MRI probes, soil bioremediations, etc. (Martinez et al. 2019). The presence of melanin plays an irreplaceable role in human lives, wherein the absence of melanin can lead to diseases like cancer, vitiligo, Waardenburg syndrome, etc. Despite such promising and diverse attributes, the complete potential of melanin is not harvested because of its heterogeneous nature, resulting in a lack of specific genetic makeup responsible for melanin biosynthesis and sequential metabolic pathways. Further, the capabilities of microbes to employ multiple precursors like tyrosine and DOPA for melanin synthesis ultimately leads to a complex process of biosynthesis (Cao et al. 2021). The isolation and complete characterization of melanin is very difficult because of its insolubility in organic solvents. The narrow-spectrum solubility of melanins makes the extraction process costly and hence reduces its industrial production (Borovansky and Riley 2011; Sun et al. 2016). As a result of such physical problems, the isolation of melanin from eukaryotic sources is hindered; in such conditions, microbial melanin can pave the way (Pavan et al. 2020; Sun et al. 2016). Culturing aspects of microbial melanin makes them feasible for easier upscaling for commercial production and efficient utilization in various sectors.

2 Extraction of Melanin

Due to the amorphous nature and structural diversity, extraction of melanin employs different methods which highly rely on factors like melanin source (fungal, bacterial, human hair) and its cellular localization (intracellular/extracellular) (Aghajanyan et al. 2005, 2017; Gómez-Marín and Sánchez 2010; Tarangini and Mishra 2014). For example, extracellular melanin extraction involves acid precipitation (Choi 2021), whereas intracellular melanin extraction employs alkali extraction, acid precipitation, ultrasonic-assisted extraction (Hu et al. 2015; Zou et al. 2010), and microwave-assisted extraction (Lu et al. 2014). The most conventional method for melanin extraction is alkali extraction and acid precipitation as melanins normally solubilize in alkaline solutions and precipitate as sediments in acidic solutions (Lu et al. 2014; Sajjan et al. 2010; Sun et al. 2016). Many alkali solutions such as sodium hydroxide, potassium hydroxide, ammonium hydroxide, calcium hydroxide, etc. are reported to be used at different concentrations of 0.1, 0.5, 1, 1.5, and 2 N for melanin extraction, whereas for precipitation purposes, double strength acid like HCl is used under slow magnetic stirring conditions. Many research groups have employed this conventional method to extract melanin from different microbial sources as summarized in review articles (Singh et al. 2021; Choi 2021). Apart from alkali extraction assisted with ultrasonication/microwave, an enzymatic method is also used for extraction of intracellular melanin due to the ability of enzymes to increase hydrolysis as well as degradation of impermeable cell walls. This method mainly utilizes specific cell wall lysing enzymes such as guanidine thiocyanate for protein denaturation and a serine proteinase for cleavage (Dadachova et al. 2007; Youngchim et al. 2004). This traditional method is economically feasible but has low extraction efficiency and is time-consuming; so nowadays there is a trend for advanced cavitation-based extraction methods which minimize the use of toxic solvents, improve extraction yield, shorten extraction duration, and use green solvents that are recycled and reusable (Ghadge et al. 2022; Panda and Manickam 2019; Zou et al. 2010). For example, melanin is extracted from *Streptomyces hyderabadensis* 7VPT5-5R using tetrabutylammonium hydroxide (40% w/w TBAOH in water) solvent which led to a 66% increase in the yield of melanin in comparison to the conventional method of extraction (Ghadge et al. 2022).

Cavitation is a phenomenon where a small low-pressure vapor-filled cavity is formed due to a rapid change in pressure under the liquid medium. Based on this phenomenon, various cavitation-based extraction techniques such as ultrasound-assisted extraction (UAE), negative-pressure cavitation (NPC) extraction, microwave-assisted extraction (MAE), and hydrodynamic cavitation extraction (HCE) have been reported (Lu et al. 2014; Zou et al. 2010). In 2010, melanin from *A. auricula* fruit bodies was extracted using cavitation-based UAE (ultrasound-assisted extraction) technology due to its numerous benefits in comparison to conventional ones such as improved extraction yield, reduced power consumption, and extraction time (Zou et al. 2010). UAE employs ultrasound pressure waves due to the resulting energy generated from these collapsing cavitational

bubbles that provide greater penetration of the solvent into the cellular material and increases mass transfer to and from interfaces. This also causes disruption of cell walls and the release of cellular materials that ultimately leads to increased extraction yield. In UAE, cavitation occurs due to the passage of ultrasound waves in the liquid medium. Whereas if it occurs, due to the pressure variations in the flowing liquid concerning the change in the geometry of constriction, then it is called hydrodynamic cavitation extraction (HCE). The limitations associated with UAE are attenuation of ultrasound waves for highly concentrated dispersed phases and lack of uniformity for dispersed extract materials (Panda and Manickam 2019). In the case of NPC, the creation of negative pressure governs cavitation. NPC extraction proved to be more effective in the extraction of heat-sensitive compounds such as polyphenols and polysaccharides (Panda and Manickam 2019). MAE uses microwave energy to heat solvents in contact with a sample to partition analytes from the sample matrix into the solvent (Lu et al. 2014; Tatke and Jaiswal 2011), but a problem with this technique is the rapid increase in temperature of the extraction mixture that may terminate the extraction process early due to the boiling of the solvent. Thus, the desired compounds are not sufficiently diffused from the material into the solvent and consequently, the extraction yield is reduced (Chuyen et al. 2018). The UAE method was reported to yield 37.33% pure melanin (Hou et al. 2019), whereas another study reported that a purification yield of 11.08% could be achieved through an MAE method, which was 40.43% higher than that obtained by alkali extraction and acid precipitation (Lu et al. 2014).

Due to the presence of various biological sources for production, structural diversity, amorphous nature, and insolubility of melanin have resulted in the non-availability of a standard method for extraction and purification of melanin. But the above-described modern extraction techniques can be alternatively used owing to numerous advantages over conventional methods like reduced energy and solvent consumption, increase in extraction yield, improvement of extract quality, reduction in extraction time, and protection of thermo-labile compounds in the extract (Panda and Manickam 2019; Tatke and Jaiswal 2011; Zou et al. 2010).

3 Purification of Melanin

Purification of melanin can be achieved by performing different steps such as redissolution, centrifugation, acid hydrolysis, precipitation, boiling, dialysis, and column chromatography followed by successive washing steps with organic solvents such as chloroform, petroleum ether, ethyl acetate, acetone, or absolute ethanol (Aghajanyan et al. 2005; Choi 2021; Dong and Yao 2012; Madhusudhan et al. 2014; Selvakumar et al. 2008; Suryanarayanan et al. 2004). Acid hydrolysis is usually performed using 6 M HCl to remove impurities like carbohydrates and protein associated with melanin pigment, whereas organic solvent aid helps in the removal of secondary metabolites. Non-hydrolyzable melanin are redissolved in NaOH and precipitated out with HCl followed by several washing steps with organic solvent

and deionized water. An additional boiling step helps to avoid the formation of melanoidins (Eskandari and Etemadifar 2021). Dialysis was reportedly used to remove salt and other impurities like low molecular weight organic and inorganic compounds (Wibowo et al. 2022). Finally, washing with absolute ethanol removes water molecules with the melanin pigment. The resulting content is lyophilized and stored as pure melanin. In 2022, one research group purified melanin with help of dialysis tubing and the resulting melanin yield was 670 mg/L, which was significantly higher than the 116 mg/L obtained from the acid precipitation method (Wibowo et al. 2022). The combination of the above-described extraction technologies has been observed to bring synergistic extraction yield compared to the conventional method paving way for the development of more advanced and efficient techniques for melanin extraction and purification.

4 Preliminary Confirmation of Melanin

The melanin pigment is insoluble in water and almost all inorganic/organic solvents. Based on this observation, a solubility test is used for the preliminary confirmation of melanin. Melanin is slightly soluble in dimethyl sulphoxide (DMSO), in water at alkaline pH, phosphate saline buffer (pH 7.2), and on the other hand, melanin gets precipitated at acidic conditions (pH 2) (Kamarudheen et al. 2019; Pralea et al. 2019). Melanin contains different functional groups in the structure like catechol, NH, and COOH that shows reactivity with certain chemicals and shows distinguishable characters helping in the identification of melanin type. When melanin is treated with hydrogen peroxide (H_2O_2), it results in decolorization due to oxidative degradation of melanin. In this reaction, the nucleophilic attack of OOH^- ions from H_2O_2 leads to the production of quinone epoxide causing bleaching of melanin (Korytowski and Sarna 1990). The reduction of $AgNO_3$ occurs when it reacts with microbial melanin leading to the formation of gray colour on the walls of the test tube due to the precipitation of melanin (Carriel et al. 2011; Lopusiewicz 2018). Similarly, when melanin reacts with $KMnO_4$, it leads to a change in color from brown to green with precipitation and decoloration of the solution. The color change is due to the reduction of $KMnO_4$ by the redox property of melanin. This reaction indicates the presence of quinone and phenol groups in the structure of melanin (Aghajanyan et al. 2005).

Chemical degradation methods are also used in the identification of different types of melanins based on the analysis of their degradation products. Melanin gets degraded by strong oxidants and reductants yielding different types of degraded products. These degraded products are further separated by chromatographic techniques and identification by different spectroscopic techniques (Dzierżęga-Lęcznar et al. 2002). Generally, gas chromatography and mass spectrometry with pyrolysis (Py-GC/MS) are used to identify pyrrole, indole, and their alkyl derivatives as pyrrole di- and tricarboxylic acids are precursors of eumelanin biosynthesis (Dzierżęga-Lęcznar et al. 2002, 2012). Likewise, in the case of pheomelanin,

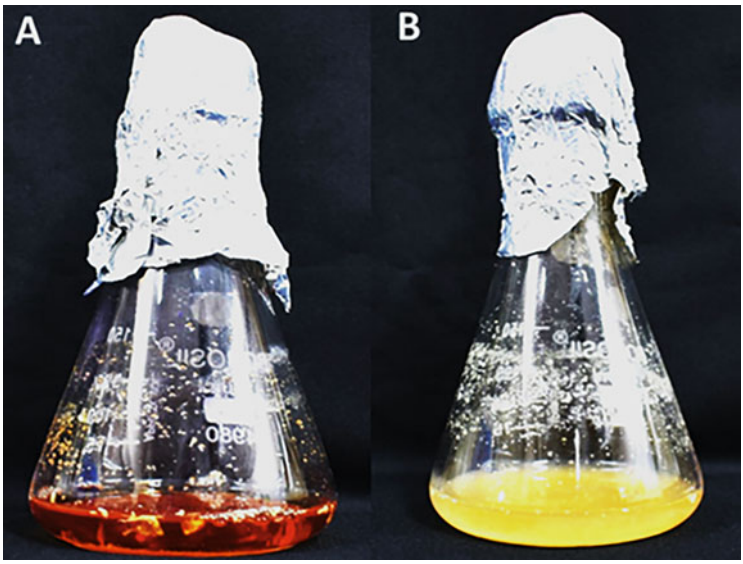

Fig. 1 Melanin synthesis inhibition: control (**a**) and treatment with kojic acid (**b**) (Ghadge et al. 2022)

precursors are thiazole or benzothiazole carboxylic acids including some other melanin pigment markers, i.e., isomeric aminohydroxyphenylalanines and aminohydroxyphenylethylamines (Donato and Napolitano 2003; Dzierżęga-Lęcznar et al. 2012; Greco et al. 2009; Ito et al. 2019).

The melanin synthesis inhibition is used to identify the enzyme involved in melanin biosynthesis by the producer strain and type of melanin. The most commonly used inhibitors are kojic acid as a tyrosinase inhibitor, tricyclazole as a DHN-melanin inhibitor, and sodium azide as a laccase inhibitor. Inhibition of melanin synthesis by kojic acid was observed for strains *Actinoalloteichus sp.* MA-32, *Streptomyces hyderabadensis* 7VPT5-5R (Fig. 1) (Ghadge et al. 2022; Manivasagan et al. 2013). The inhibition of melanin-like pigments by sodium azide was previously reported for *Bacillus weihenstephanensis*, *Bacillus subtilis* 4NP-BL (Fig. 2) (Drewnowska et al. 2015; Ghadge et al. 2020). A higher concentration of sodium azide (>50 μg mL^{-1}) led to the inhibition of bacterial growth. The inhibition of melanin synthesis is reported in the black yeasts *Trimmatostroma salinum*, *Phaeotheca triangularis* and *Hortaea werneckii* by use of tricyclazole, a specific inhibitor for polyketide melanin biosynthesis (Kogej et al. 2003).

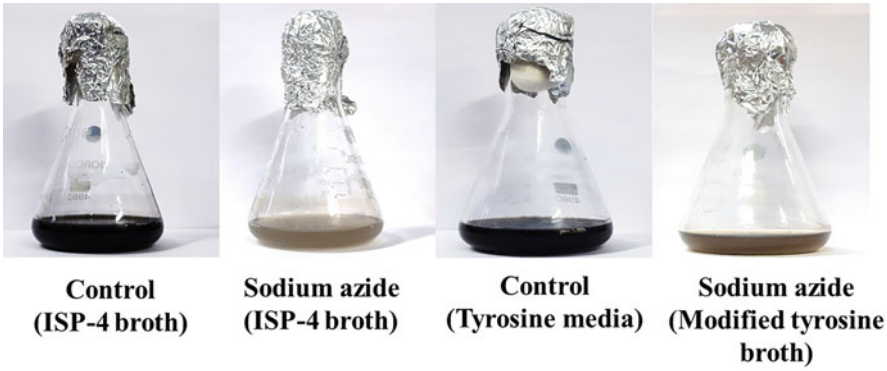

Fig. 2 Inhibition of melanin synthesis by sodium azide (Ghadge et al. 2020)

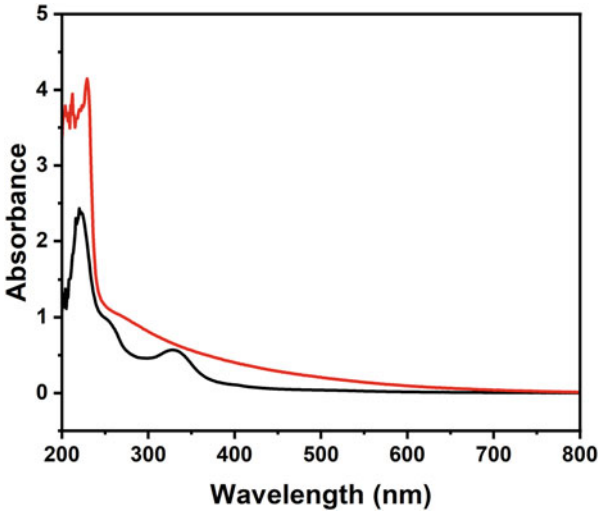

Fig. 3 UV/vis spectra of purified melanin (black) and synthetic melanin (red) (Ghadge et al. 2022)

5 Characterization of Melanin

5.1 UV–Visible Spectroscopy

UV/visible spectroscopy is the most common and widely accepted technique used for the primary identification/confirmation of melanin. The absorbance of melanin monotonically increases towards the UV region (high energy). It decreases towards the visible region (low energy radiation), which is a unique characteristic property found in melanin and this property is employed for melanin identification (Fig. 3) (Gao and Garcia-Pichel 2011). Melanin of microbial origin shows maximum absorption in the almost entire UV region (200–400 nm). The ratio of A_{650}/A_{500} is used to quantify eumelanin concentration from the mixture as well as for the differentiation

of eumelanin and pheomelanin. The ratio of melanin above 0.25 is referred as eumelanin, while a ratio below 0.15 is considered pheomelanin (Saini and Melo 2015).

As we know, photoprotection is the main function of eumelanin and it is due to broadband absorption, but its origin is still mysterious. The recent theoretical (computational) and experimental studies indicated that broadband absorption emerges from the chemical disorder of eumelanin due to the chemical diversity of building blocks at the oligomeric level and it is widely accepted (Singh et al. 2021). Based on previous studies, the oligomeric model is most acceptable for the origin of broadband absorption due to the formation of different types of chemically-modified oligomers having different configurations and conformations. These oligomers interact with each other mainly by π–π interactions, which affect the electron delocalization resulting in the absorption spectrum of eumelanin (Arzillo et al. 2012). The different studies speculated that non-covalent interactions play a major role during eumelanin oligomerization in multilevel structural organization, like stacking interactions (π–π) (Chen et al. 2013). The close association of oligomers in a multilevel organized structure determines the alteration of absorption spectra. DHI and DHICA precursors are used to study the aggregation model of eumelanin and its UV/VIS properties to understand broadband absorption (Ju et al. 2018). Their investigation revealed that monomeric units (DHI and DHICA) undergo polymerization from monomer to oligomers and then oligomers form small stacks. These stacked oligomers further oligomerize and stacked to form larger aggregates called protomolecules (Spano 2010). Their findings provided strong support to postulate that broad absorption bands due to delocalization of intrinsic π-electron within integral eumelanin oligomers and altered by other interactions such as attractive stacking between aromatic rings and aggregation in the stratified framework of complex structure (Simpson et al. 2014).

The recent studies on eumelanin supported the hypothesis of an aggregate model of eumelanin but its detailed structure is still unknown due to a lack of experimental proof. Because eumelanin precursor is redox-active and has different polymeric sites it makes it very difficult to understand its structure-property relationship. The complexity and heterogeneity of eumelanin hinder the experimental approaches to understanding its structural and optical properties (Yildirim and Bayindir 2014).

5.2 Electron Paramagnetic Resonance (EPR)

"Paramagnetism" is one of the main fundamental properties of eumelanin. Eumelanin is a redox-active macromolecule due to the presence of indolequinone group precursor molecule 5,6-dihydroxyindole (DHI) and 5,6-dihydroxyindole-2-carboxylic acid (DHICA). Eumelanin contains different paramagnetic centers, which is due to quinone groups in the structure (Gessler et al. 2014). Recent studies on eumelanin identified two types of paramagnetic centers in solid-state- and liquid-state. These centers are differentiated from each other by their *g*-factors and

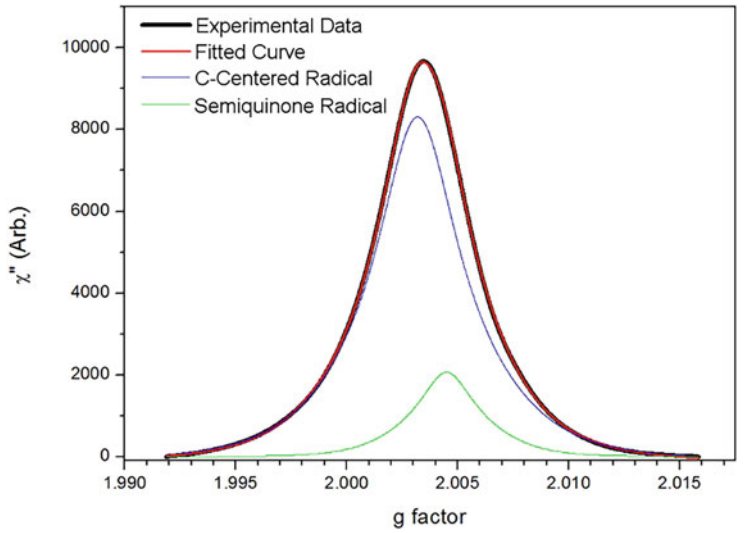

Fig. 4 Deconvolution of the integrated EPR spectrum associated with the basic sample. The spectrum is best explained by the presence of two free radicals, the more dominant carbon-centered signal ($g = 2.0032$) and the small semiquinone signal ($g = 2.0045$). Data at a water content of 14.0% and microwave power of 0.71 mW1/2 (Mostert et al. 2013)

line shapes (Paulin et al. 2019). It is hypothesized that carbon-centered radicals (CCR) come from the internal skeleton of the eumelanin structure, and it is prevented by the external environment (Paulin et al. 2021a). CCRs were mainly found in solid samples (dry powder) and they are less affected by temperature and pH. The semiquinone free radicals (SFR) are observed in the liquid state (solution) and strongly affected (change in intensity of signal) by pH. Furthermore, these two types of free radicals have constant *g*-factors, 2.003 for CCR and 2.005 for SFR (Fig. 4).

Paulin et al. 2019 performed experimental and theoretical work on the paramagnetic behavior of melanin. They used a computational model (DFT) to compare *g*-factors and hyperfine coupling constants to correlate the structure and free radical centers of melanin. The precursors of eumelanin, DHI, and DHICA, are redox-active molecules with different redox states (Fig. 5), containing both positive and negative charged states having an unpaired electronic and zwitterionic state of an odd number of electrons (Cuba et al. 2021).

The results show that the partially oxidized molecules (indolequinone and semiquinone) are associated with semiquinone free radicals (SFR), while fully reduced state (hydroquinone) and nitrogen-protonated species (DHICA) are associated with carbon-centered radicals (CCR). The positively charged species are referred to as a secondary product of eumelanin and such types of species are found in eumelanin derivatives (Paulin et al. 2019). The results revealed that the

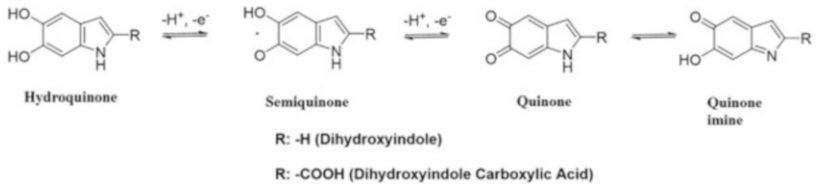

Fig. 5 Different redox forms of melanin monomeric structures: R = H (DHI) or COOH (DHICA) (Reali et al. 2021)

presence of three types of EPR signals comes from typical eumelanin structures. Based on experimental data, it is observed that the EPR signals of CCR from two precursors DHI and DHICA can be differentiated. In this work, the main focus was on the differentiation of paramagnetic species present in eumelanin. The experimental results of EPR spectra of eumelanin and its precursor molecules (DHI and DHICA) revealed that it contains three different types of free radicals, among them, two are CCRs and another is SFR. Investigation of EPR variables and energy state of different substructures of eumelanin indicated that the carbon-centered radicals (CCRs) mainly come from the reduced state of eumelanin structural organization (Paulin et al. 2019, 2021a).

Eumelanin is associated with the presence of *O*-semiquinone radicals, while pheomelanin contains *O*-semiquinoneimine radicals. EPR spectrum can distinguish different types of melanins, eumelanin shows a single line with a hyperfine shape at variable temperature (low to high) and is less affected by microwave power, while that of pheomelanin has a complex line shape with hyperfine structure arising through the interplay between free electrons with electrons of adjacent nitrogen nuclei (Zdybel et al. 2017). Natural melanin can be differentiated from synthetic melanin by observing spectral patterns and line width. These characteristic differences in line shape and width of the EPR spectrum were used to distinguish natural melanin from synthetic melanin.

5.3 Electrical Properties of Melanin

Melanin has two main properties, broadband absorption, and redox activity, which are responsible for electric charge conduction. The property of melanin to conduct electrical charge was studied in the 1970s, and its semiconducting charge behavior was demonstrated by Mott-Davis amorphous semiconductor (MDAS) theory (McGinness 1972; McGinness et al. 1974; Powell and Rosenberg 1970). The electric conductivity of melanin is due to the presence of different functional groups (carboxylates, aromatic amines, and catechols) having different redox states which generate protons and electrons during oxidation-reduction reactions. The various types of charge transport mechanisms are reported to be present in eumelanin i.e. intra- and inter-atomic interaction (H-bonding), and π–π interaction (Gouda

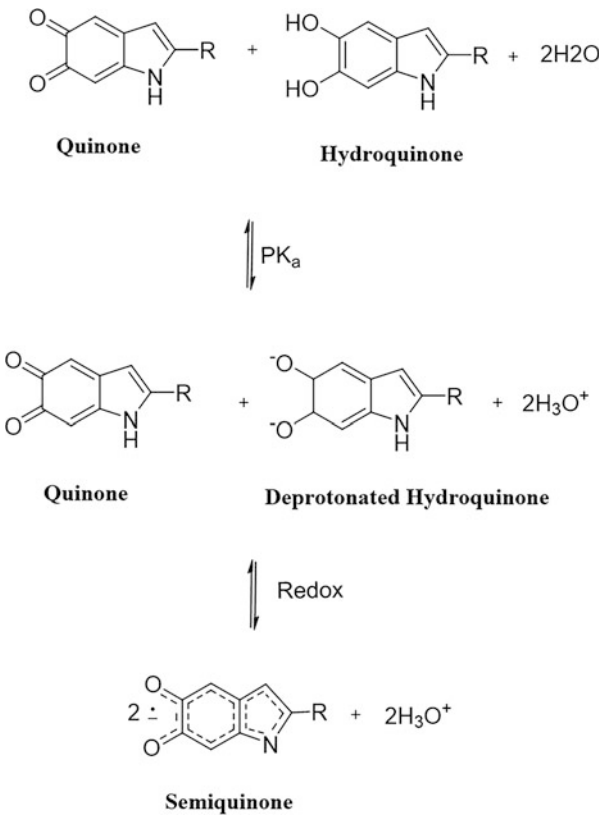

Fig. 6 The comproportionation equilibrium reaction involves two steps: hydroquinone deprotonates leading to hydronium formation; and the hydroquinone reacts with a quinone in a 1-electron redox reaction to form semiquinone radicals, a moiety of an intermediate oxidative state (Sheliakina et al. 2018)

et al. 2020). The current charge transport model of melanin was explained by comproportionation equilibrium (Fig. 6), where quinone and hydroquinone species react in the presence of water to generate semiquinone species and protons. From recent work, it is observed that the previous amorphous semiconductor model is replaced by the comproportionation equilibrium model in which the formation of free radicals (electron) and hydronium ions (protons) takes place where hydronium ions are mobile charge carriers showing hybrid ionic-electronic behavior (Mostert et al. 2012; Sheliakina et al. 2018; Tian et al. 2019).

5.4 Fourier-Transform Infrared Spectroscopy (FT-IR)

FT-IR spectroscopy utilizes the infrared part of the spectrum comprising wavelengths from 4000 to 700 cm^{-1}. Absorption of a specific wavelength in the infrared spectrum is a characteristic of functional groups. This absorption in the infrared spectrum varied by wavelength and intensity is measured by FT-IR spectroscopy and these details are used to detect the presence of different functional groups in

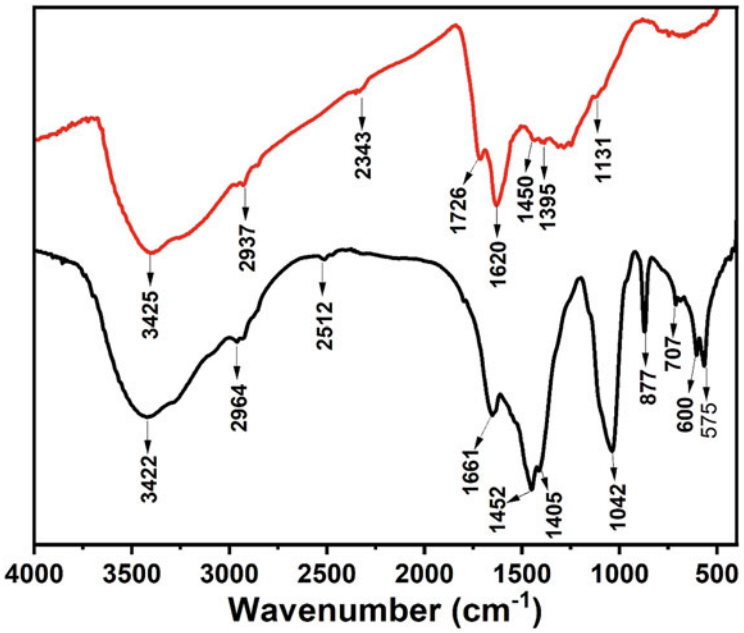

Fig. 7 FT-IR spectra of purified melanin (black) and synthetic melanin (red) (Ghadge et al. 2022)

given samples (Mbonyiryivuze et al. 2015). The complexity of melanin structure made it difficult to study using spectrometry techniques. Melanin has functional groups like amides, hydroxy, carboxylic, phenolics, aromatic rings, aliphatic carbon, and indole ring. Given the different functional groups present in the melanin, FT-IR can serve as a technique for the identification of melanin, detection of impurity, metal conjugation, and type of melanin (Sajjan et al. 2013). A careful investigation of the literature reveals some signature patterns of melanin in IR spectra. A broad peak of O–H and N–H stretching in the range of 3600–2800 cm^{-1}, a sharp peak due to stretching of CH_3 group in the range of 2900–3000 cm^{-1}. In some cases of eumelanin, CH_3 and CH_2 stretching absorption give 2 to 3 peaks in the range of 2800–3000 cm^{-1}, these peaks are generally small and fall in the broad peak of O–H and N–H stretching. Stretching of C=O, C=C, and COO– represented by a sharp deep peak in the range of 1620–1650 cm^{-1}. Next to this small peak in the range of 1500–1600 cm^{-1}, there is a characteristic peak of melanin having an indole ring due to the bending of the N–H group. Other characteristic peaks of melanin in the range of 1400–1500 cm^{-1} are due to aliphatic carbons. In this range, peaks appear due to C–H, CH_2–CH_3 bending vibration. The phenolic stretching vibration of microbial melanin gives a small peak in the range of 1200–1300 cm^{-1}. Weak peaks in the range of 900–600 cm^{-1} are due to N–H wagging, aromatic C–H, and the substitution of alkene C–H (Ammanagi et al. 2021; El-Naggar and El-Ewasy 2017; Ghadge et al. 2020; Vasanthabharathi et al. 2011) (Fig. 7).

5.5 X-Ray Photoelectron Spectroscopy (XPS)

XPS is used to analyze the elemental composition and state of elements on the surface of the solid samples. Due to the problems in solubility of the melanin, XPS is quite a handy technique to analyze the composition, hybridization, oxidation state of elements, and conformation of functional groups present in the melanin. To analyze the average surface chemistry of the sample, XPS uses low energy X-ray (Soft X-ray). This low-energy photon then generates a photoelectron from the atoms present on the sample surface. Thus, XPS utilizes the difference in the binding energy of the electrons in different atoms by measuring the kinetic energy of the photoelectron emitted from the sample surface and uses this data to generate the information about surface chemistry of the sample (Van der Heide 2011).

Selection of the energy range of photoelectrons allowed screening of one element at a time. Each atomic orbit of every element has characteristic binding energy, thus giving a specific peak for every atom. The binding energy of electrons depends on the chemical and physical environment of the atom. This helps in the identification of different types of bonds formed by elements in the material. For example, in the process of screening of C1s photoelectron, the presence of C–O–C, C=O, C=OH, –O–C=O, –O–CO–O will cause the sifting of the peak, while the main peak consists of signals of C–C, C=C, and CH (Bregadiolli et al. 2021). The values for different states of elements or chemical shifts are available in databases like 'The International XPS Database' (https://xpsdatabase.com/).

A study on the eumelanin from four different sources using XPS gives an insight into the structure of the composition and structural differences among them. Elemental composition of the natural eumelanin from sepia, crow feather, turkey feather, and human hair gives us a range of composition in eumelanin like carbon 66.3–67.4%, oxygen 18.8–22.2%, and nitrogen 8.7–12.9%. Natural eumelanin is made up of DHI, DHICA, and their derivatives, so the calculation of the ratio between C=O and O–C=O and the amount and concentration of O–C=O is directly equal to the amount of DHICA and its oxidized forms of monomers. The scanning of the C1s will give the largest peak at 285 eV, peak fitting of this peak can be done using chemical shifts for C–C(H) at 284.9 + 0.2 eV, C–OH/C–N 286.3 + 0.2 eV, C=O at 288.1 + 0.2 eV, O–C=O at 289.3 + 0.2 eV approximately (Xiao et al. 2018).

The surface layer of the material is susceptible to absorption of water, CO, and oxidative modification, which can result in the wrong quantification of the composition of melanin. The problem of surface modification can be eliminated by a cluster beam of 500 Argon ions (Paulin et al. 2021b).

5.6 Raman Spectroscopic Analysis

Peak around 1590 cm^{-1} denoted the stretching vibrations of aromatic C=C bond in the indole ring. Bands around 1690 cm^{-1} arise due to quinone C=O stretching.

Signals around 1510 cm^{-1} are related to the C=N stretching. The band around 1341 cm^{-1} is observed due to aromatic C–N stretching of the indole structure. C–O stretching of the carboxylic acid is visible at about 1220 cm^{-1} (Capozzi et al. 2005).

Four bands were found to be visible in the spectrum of pheomelanin in the range of 500–2000 cm^{-1}. A band around wavenumber 500 cm^{-1} is considered an out-of-plane deformation of the phenyl ring in the benzothiazine structure. The stretching vibrations of the C–N bond are also observed in pheomelanin at about 1150 cm^{-1}. Stretching vibrations of phenyl ring arise in the Raman spectrum at around 1490 cm^{-1}. High Raman intensity in the range of 1750–2000 cm^{-1} is considered the characteristic pattern for the pheomelanin because eumelanin shows a flat line in this region (Galvan et al. 2013).

5.7 *Nuclear Magnetic Resonance (NMR) Spectroscopy*

There are four major classes of melanin named eumelanin, pheomelanin, allomelanin, and pyomelanin. The basic moiety of the eumelanin structure is comprised of 5,6-dihydroxy indole (DHI) and 5,6-dihydroxy indole carboxylic acid (DHICA). The monomeric unit in the pheomelanin is composed of a benzothiazine ring. Allomelanin is made up of the 1,8-dihydroxy naphthalene moiety. These structural differences within the different types of melanin are observed due to variations in the precursor moiety or intermediate compounds during melanin production. Spectroscopic data is important to study the structural characteristics of melanin. ^{1}H NMR and ^{13}C NMR are widely used techniques to determine the structural features of melanin.

^{1}H NMR spectrum of eumelanin showed prominent peaks of resonance around 7.286 and 7.21 ppm (Fig. 8) which are attributed to the indole/pyrrole ring. –NH groups of melanin moiety give signals around 8.00 ppm as a singlet. Peaks in the range of 3.4 and 4.4 ppm are ascribed to the protons attached to the methyl or methylene group, which are attached to nitrogen and/or oxygen atoms. Signals at 2.2 and 2.8 ppm provide evidence for the presence of the methylene group. Signals at 1.00 and 3.00 ppm denoted the presence of the –NH group lined to the indole. Resonance signals around 0.9–1.00 ppm are described for aliphatic fragments such as CH_2CH_3 and $CH(CH_3)_2$ (Barretto and Vootla 2020; Ghadge et al. 2020). In the ^{13}C NMR spectrum, peaks in the range of 120–140 ppm are due to the aromatic carbons involved in the indole or pyrrole system. The peaks from 50–60 ppm arise due to the carbon atom linked to the nitrogen. The peaks for the methyl and methylene groups are observed within the 10–40 ppm range.

^{13}C NMR spectra of pheomelanin show characteristic peaks from 30–70 ppm which resemblance to = C–S and C–H from the aliphatic chain present in cysteine. Resonance around 170–200 ppm is attributed to the carbonyl carbon. Signals around 110–160 are observed in the spectra indicating the presence of aromatic carbons (De Souza et al. 2018).

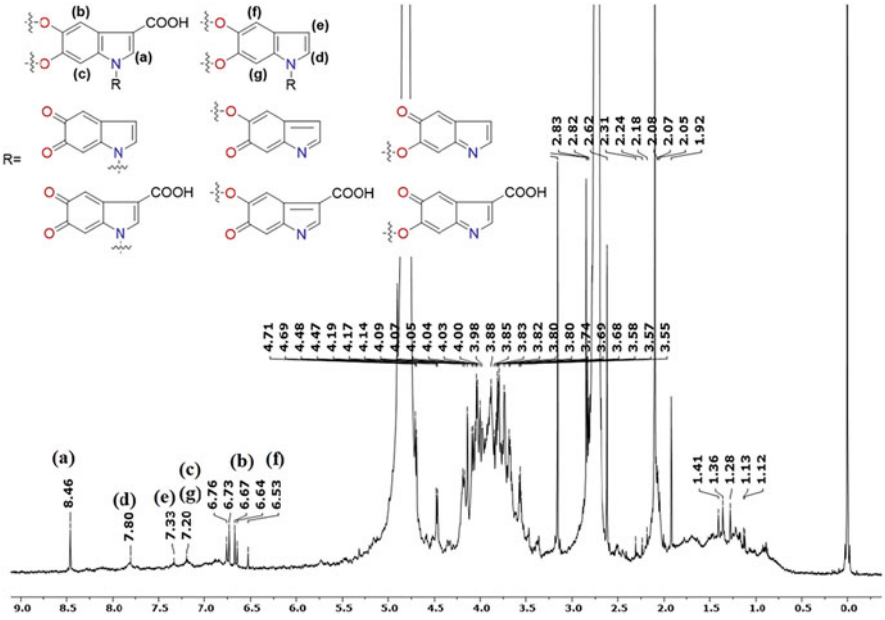

Fig. 8 ^{1}H NMR spectrum of the purified melanin (Ghadge et al. 2022)

In the past literature, allomelanin was characterized by Cross-Polarization Magic-angle spinning (CP/MS) NMR spectroscopy. ^{13}C spin echo (SE) CP/MAS NMR spectrum shows a broad range of peaks from 100 to 160 ppm due to the presence of protonated and non-protonated aromatic carbons. Peaks in the range of 20–40 ppm are due to the protonated aliphatic carbon (Singla et al. 2021). A characteristic peak of phenoxy carbon can also be found at around 152 ppm in the solid-state NMR (Zhou et al. 2019).

6 Conclusion

Microorganisms can produce different types of melanin and utilize a variety of precursor molecules for synthesis. Heterogeneity due to different sources, metabolic pathways, and precursor molecules has resulted in the complex supramolecular structure of melanin. Microbial melanin has gained interest due to its diverse functions within the host and various biological activities and also it has an advantage over other sources of melanin for production due to scalability, sustainability, and cheaper production cost. Despite such importance of melanin, its commercial utilization is restricted due to its insolubility, and low yield which results in higher production costs. The extraction and purification of melanin is a difficult job due to its diverse origin, location, and complex structure. So, there is an urgent need to

develop sustainable extraction methods which will increase the yield and solubility of melanin. The complexity and heterogeneity of melanin are the main hurdles for structure elucidation, which will need the use of different modern analytical techniques and approaches. This book chapter covers microbial melanin production, extraction techniques, and its structural properties through different analytical techniques. Due to the multifunctionality and biocompatibility of melanin, it has become a tunable biomaterial of application in various fields. Still, the fundamental structural-property relationship is not fully understood which will attract the researchers and has scope for further development.

Acknowledgments Vishal Ghadge thanks SERB-DST for a project fellowship (GAP-2050 and GAP-2057), Sanju Singh, Doniya Elze Mathew, Asmita Dhimmar acknowledges CSIR-JRF fellowship from the Council of Scientific and Industrial Research (CSIR), Pankaj Kumar and Apexa Gajjar acknowledges DBT-JRF fellowship from Department of Biotechnology (DBT), and Harshal Sahastrabudhe acknowledges GATE-JRF fellowship from Council of Scientific and Industrial Research (CSIR).

Funding This research was supported by the Scientific and Engineering Research Board (SERB), Department of Science and Technology [ECRA/2016/000788 and EEQ/2016/000268]; and Council of Scientific and Industrial Research [MLP/0027].

References

Abbas M, D'Amico F, Morresi L, Pinto N, Ficcadenti M, Natali R, Ottaviano L, Passacantando M, Cuccioloni M, Angeletti M, Gunnella R (2009) Structural, electrical, electronic and optical properties of melanin films. Eur Phys J 28:285–291

Aghajanyan AE, Hambardzumyan AA, Hovsepyan AS, Asaturian RA, Vardanyan AA, Saghiyan AA (2005) Isolation, purification and physicochemical characterization of water-soluble *Bacillus thuringiensis* melanin. Pigment Cell Res 18:30–135

Aghajanyan AE, Vardanyan AA, Hovsepyan AC, Hambardzumyan AA, Filipenia V, Saghyan AC (2017) Development of technology for obtaining water-soluble bacterial melanin and determination of some of pigment properties. Biotechnologia 98:315–322

Ammanagi A, Shivasharana CT, Badiger A, Ramaraj V (2021) Functional and structural characterization of melanin from *Brevibacillus invocatus* strain IBA. Dokl Biol Sci 500:159–169

Arzillo M, Mangiapia G, Pezzella A, Heenan RK, Radulescu A, Paduano L, d'Ischia M (2012) Eumelanin buildup on the nanoscale: aggregate growth/assembly and visible absorption development in biomimetic 5,6-dihydroxyindole polymerization. Biomacromolecules 13:2379–2390

Barretto DA, Vootla SK (2020) Biological activities of melanin pigment extracted from Bombyx mori gut-associated yeast *Cryptococcus rajasthanensis* KY627764. World J Microbiol Biotechnol 36:159

Borovansky J, Riley PA (2011) Melanins and melanosomes: biosynthesis, structure, physiological and pathological functions. Wiley-VCH, Australia

Bothma JP, De Boor J, Divakar U, Schwenn PE, Meredith P (2008) Device quality electrically conducting melanin thin films. Adv Mater 20:3539–3542

Bregadiolli BA, Paulin JV, Albano LGS, Martins LM, De Camargo DHS, da Silva-Filho LC, Bufon CCB, de Oliveira Graeff CF (2021) A strategy towards melanin-based functional material: rGO and sulfonated melanin composites. J Mater Chem C 9:16991–17002

Cao W, Zhou X, McCallum NC, Hu Z, Ni QZ, Kapoor U, Heil CM, Cay KS, Zand T, Mantanona AJ, Jayaraman A, Dhinojwala A, Deheyn DD, Shawkey MD, Burkart MD, Rinehart JD, Gianneschi NC (2021) Unraveling the structure and function of melanin through synthesis. J Am Chem Soc 143:2622–2637

Capozzi VITO, Perna G, Gallone A, Biagi PF, Carmone P, Fratello A, Guida G, Zanna P, Cicero R (2005) Raman and optical spectroscopy of eumelanin films. J Mol Struct 744:717–721

Carriel VS, Aneiros-Fernandez J, Arias-Santiago S, Garzón IJ, Alaminos M, Campos A (2011) A novel histochemical method for a simultaneous staining of melanin and collagen fibers. J Histochem Cytochem 59:270–277

Chen CT, Ball V, de Almeida GJJ, Singh MK, Toniazzo V, Ruch D, Buehler MJ (2013) Self-assembly of tetramers of 5,6-dihydroxyindole explains the primary physical properties of eumelanin: experiment, simulation, and design. ACS Nano 7:1524–1532

Choi KY (2021) Bioprocess of microbial melanin production and isolation. Front Bioeng Biotechnol 9:765110

Chuyen HV, Nguyen MH, Roach PD, Golding JB, Parks SE (2018) Microwave-assisted extraction and ultrasound-assisted extraction for recovering carotenoids from Gac peel and their effects on antioxidant capacity of the extracts. Food Sci Nutr 6:189–196

Cuba JP, Alves GG, Galindo LA, Paulin JV, Batagin-Neto A (2021) Sulfonated melanin derivatives: theoretical evaluation of local reactivities and chemical structures. J Mol Model 27:362

Dadachova E, Bryan RA, Huang X, Moadel T, Schweitzer AD, Aisen P, Nosanchuk JD, Casadevall A (2007) Ionizing radiation changes the electronic properties of melanin and enhances the growth of melanized fungi. PLoS One 2:e457

De Souza RA, Kamat NM, Nadkarni VS (2018) Purification and characterisation of a Sulphur rich melanin from edible mushroom *Termitomyces albuminosus Heim*. Mycology 9:296–306

Donato PD, Napolitano A (2003) 1,4-Benzothiazines as key intermediates in the biosynthesis of red hair pigment pheomelanins. Pigment Cell Res 16:532–539

Dong C, Yao Y (2012) Isolation, characterization of melanin derived from *Ophiocordyceps sinensis*, an entomogenous fungus endemic to the Tibetan Plateau. J Biosci Bioeng 113:474–479

Drewnowska JM, Zambrzycka M, Kalska-Szostko B, Fiedoruk K, Swiecicka I (2015) Melanin-like pigment synthesis by soil *Bacillus weihenstephanensis* isolates from Northeastern Poland. PLoS One 10:e0125428

Dzierżęga-Lęcznar A, Chodurek E, Stępień K, Wilczok T (2002) Pyrolysis-gas chromatography-mass spectrometry of synthetic neuromelanins. J Anal Appl Pyrolysis 62:239–248

Dzierżęga-Lęcznar A, Kurkiewicz S, Stępień K (2012) Detection and quantitation of a pheomelanin component in melanin pigments using pyrolysis–gas chromatography/tandem mass spectrometry system with multiple reaction monitoring mode. J Mass Spectrom 47:242–245

El-Naggar NEA, El-Ewasy SM (2017) Bioproduction, characterization, anticancer and antioxidant activities of extracellular melanin pigment produced by newly isolated microbial cell factories *Streptomyces glaucescens* NEAE-H. Sci Rep 7:42129

Eskandari S, Etemadifar Z (2021) Biocompatibility and radioprotection by newly characterized melanin pigment and its production from *Dietzia schimae* NM3 in optimized whey medium by response surface methodology. Ann Microbiol 71:17

Galvan I, Jorge A, Solano F, Wakamatsu K (2013) Vibrational characterization of pheomelanin and trichochrome F by Raman spectroscopy. Spectrochim Acta A Mol Biomol Spectrosc 110:55–59

Gao Q, Garcia-Pichel F (2011) Microbial ultraviolet sunscreens. Nat Rev Microbiol 9:791–802

Gessler NN, Egorova AS, Belozerskaya TA (2014) Melanin pigments of fungi under extreme environmental conditions. Appl Biochem Microbiol 50:105–113

Ghadge V, Kumar P, Maity TK, Prasad K, Shinde PB (2022) Facile alternative sustainable process for the selective extraction of microbial melanin. ACS Sustain Chem Eng 10:2681–2688

Ghadge V, Kumar P, Singh S, Mathew DE, Bhattacharya S, Nimse SB, Shinde PB (2020) Natural melanin produced by the endophytic *Bacillus subtilis* 4NP-BL associated with the halophyte *Salicornia brachiata*. J Agric Food Chem 68:6854–6863

Gómez-Marín AM, Sánchez CI (2010) Thermal and mass spectroscopic characterization of a sulphur-containing bacterial melanin from *Bacillus subtilis*. J Non-Cryst Solids 356:1576–1580
Gosset G (2017) Biotechnological production of melanins with microorganisms. In: Singh OV (ed) Bio-pigmentation and biotechnological implementations. Wiley, pp 161–171
Gouda A, Soavi F, Santato C (2020) Eumelanin electrodes in buffered aqueous media at different pH values. Electrochim Acta 347:136250
Greco G, Wakamatsu K, Panzella L, Ito S, Napolitano A, d'Ischia M (2009) Isomeric cysteinyldopas provide a (photo) degradable bulk component and a robust structural element in red human hair pheomelanin. Pigment Cell Melanoma Res 22:319–327
Haining RL, Achat-Mendes C (2017) Neuromelanin one of the most overlooked molecules in modern medicine, is not a spectator. Neural Regen Res 12:372–375
Hou R, Liu X, Xiang K, Chen L, Wu X, Lin W, Zheng M, Fu J (2019) Characterization of the physicochemical properties and extraction optimization of natural melanin from *Inonotus hispidus* mushroom. Food Chem 277:533–542
Hu WL, Dai DH, Huang GR, Zhang ZD (2015) Isolation and characterization of extracellular melanin produced by *Chroogomphus rutilus* D447. Am J Food Technol 10:68–77
Ito S, Kolbe L, Weets G, Wakamatsu K (2019) Visible light accelerates the ultraviolet A-induced degradation of eumelanin and pheomelanin. Pigment Cell Melanoma Res 32:441–447
Ju KY, Fischer MC, Warren WS (2018) Understanding the role of aggregation in the broad absorption bands of eumelanin. ACS Nano 12:12050–12061
Kamarudheen N, Naushad T, Rao KVB (2019) Biosynthesis, characterization and antagonistic applications of extracellular melanin pigment from marine *Nocardiopsis Sps*. Indian J Pharm Educ Res 53:112–120
Kogej T, Wheeler MH, Rižner TL, Gunde-Cimerman N (2003) Inhibition of DHN-melanin biosynthesis by tricyclazole in *Hortaea werneckii*. In: Non-conventional yeasts in genetics, biochemistry and biotechnology. Springer, Heidelberg, pp 143–148
Korytowski W, Sarna T (1990) Bleaching of melanin pigments. Role of copper ions and hydrogen peroxide in autooxidation and photooxidation of synthetic dopa-melanin. J Biol Chem 265: 12410–12416
Lopusiewicz L (2018) *Scleroderma citrinum* melanin: isolation, purification, spectroscopic studies with characterization of antioxidant, antibacterial and light barrier properties. World Sci News 94:114–129
Lu Y, Ye M, Song S, Li L, Shaikh F, Li J (2014) Isolation, purification, and anti-aging activity of melanin from *Lachnum singerianum*. Appl Biochem Biotechnol 174:762–771
Madhusudhan DN, Mazhari BBZ, Dastager SG, Agsar D (2014) Production and cytotoxicity of extracellular insoluble and droplets of soluble melanin by *Streptomyces lusitanus* DMZ-3. Biomed Res Int 2014:2014
Manivasagan P, Venkatesan J, Senthilkumar K, Sivakumar K, Kim SK (2013) Isolation and characterization of biologically active melanin from *Actinoalloteichus sp*. MA-32. Int J Biol Macromol 58:263–274
Martinez LM, Martinez A, Gosset G (2019) Production of melanins with recombinant microorganisms. Front Bioeng Biotechnol 7:285
Mbonyiryivuze A, Mwakikunga BW, Dhlamini SM, Maaza M (2015) Fourier transform infrared spectroscopy for sepia melanin. Mater Chem Phys 3:25–29
McGinness J, Corry P, Proctor P (1974) Amorphous semiconductor switching in melanins. Science 183:853–855
McGinness JE (1972) Mobility gaps: a mechanism for band gaps in melanins. Science 177:896–897
Mostert A, Hanson G, Sarna T, Gentle I, Powell BJ, Meredith P (2013) Hydration-controlled X-band EPR spectroscopy: A tool for unravelling the complexities of the solid-state free radical in eumelanin. J Phys Chem B 117:4965–4972
Mostert AB, Powell BJ, Pratt FL, Hanson GR, Sarna T, Gentle IR, Meredith P (2012) Role of semiconductivity and ion transport in the electrical conduction of melanin. Proc Natl Acad Sci 109:8943–8947

Nicolaus RA (1968) Melanins. Herman Press, Paris
Panda D, Manickam S (2019) Cavitation technology—the future of greener extraction method: A review on the extraction of natural products and process intensification mechanism and perspectives. Appl Sci 9:766
Paulin JV, Batagin-Neto A, Graeff CF (2019) Identification of common resonant lines in the EPR spectra of melanins. J Phys Chem B 123:1248–1255
Paulin JV, Batagin-Neto A, Naydenov B, Lips K, Graeff CF (2021a) High-field/high-frequency EPR spectroscopy on synthetic melanin: on the origin of carbon-centered radicals. Adv Mater Sci 2:6297–6305
Paulin JV, McGettrick JD, Graeff CFO, Mostert AB (2021b) Melanin system composition analyzed by XPS depth profiling. Surf Interfaces 24:101053
Pavan ME, Lopez NI, Pettinar IMJ (2020) Melanin biosynthesis in bacteria, regulation and production perspectives. Appl Microbiol Biotechnol 104:1357–1370
Powell MR, Rosenberg B (1970) The nature of the charge carriers in solvated biomacromolecules. J Bioenerg 1:493–509
Pralea IE, Moldovan RC, Petrache AM, Ilies M, Heghes SC, Ielciu I, Nicoara R, Moldovan M, Ene M, Radu M, Uifalean A, Iuga CA (2019) From extraction to advanced analytical methods: the challenges of melanin analysis. Int J Mol Sci 20:3943
Reali M, Saini P, Santato C (2021) Electronic and protonic transport in bio-sourced materials: a new perspective on semiconductivity. Adv Mater Sci Eng 2:15–31
Saini AS, Melo JS (2015) One-pot green synthesis of eumelanin: process optimization and its characterization. RSC Adv 5:47671–47680
Sajjan S, Kulkarni G, Yaligara V, Lee K, Karegoudar TB (2010) Purification and physiochemical characterization of melanin pigment from *Klebsiella sp*. J Microbiol Biotechnol 20:1513–1520
Sajjan SS, Anjaneya O, Kulkarni GB, Nayak AS, Mashetty SB, Karegoudar TB (2013) Properties and functions of melanin pigment from *Klebsiella sp*. Microbiol Biotechnol Lett 4:60–69
Selvakumar P, Rajasekar S, Periasamy K, Raaman N (2008) Isolation and characterization of melanin pigment from *Pleurotus cystidiosus* (telomorph of *Antromycopsis macrocarpa*). World J Microbiol Biotechnol 24:2125–2131
Sheliakina M, Mostert AB, Meredith P (2018) Decoupling ionic and electronic currents in melanin. Adv Funct Mater 28:1–7
Simpson MJ, Wilson JW, Robles FE, Dall CP, Glass K, Simon JD, Warren WS (2014) Near-infrared excited state dynamics of melanins: the effects of iron content, photo- damage, chemical oxidation, and aggregate size. J Phys Chem A 118:993–1003
Singh S, Nimse SB, Mathew DE, Dhimmar A, Sahastrabudhe H, Gajjar A, Ghadge VA, Shinde PB (2021) Microbial melanin: recent advances in biosynthesis, extraction, characterization, and applications. Biotechnol Adv 53:107773
Singla S, Htut KZ, Zhu R, Davis A, Ma J, Ni QZ, Burkart MD, Maurer C, Miyoshi T, Dhinojwala A (2021) Isolation and characterization of allomelanin from pathogenic black knot fungus─a sustainable source of melanin. ACS Omega 6:35514–35522
Spano FC (2010) The spectral signatures of frenkel polarons in H- and J-aggregates. Acc Chem Res 43:429–439
Stepien K, Dzierzega-Lecznar A, Tam I, Kurkiewicz S (2013) Structure and biological activity of natural melanin pigments. In: Bramhchari G (ed) Chemistry and pharmacology of naturally occurring bioactive compounds. CRC Press, Florida, pp 211–238
Sun S, Zhang X, Sun S, Zhang L, Shan S, Zhu H (2016) Production of natural melanin by *Auricularia auricula* and study on its molecular structure. Food Chem 190:801–807
Suryanarayanan TS, Ravishankar JP, Venkatesan G, Murali TS (2004) Characterization of the melanin pigment of a cosmopolitan fungal endophyte. Mycol Res 108:974–978
Tarangini K, Mishra S (2014) Production of melanin by soil microbial isolate on fruit waste extract: two step optimization of key parameters. Biotechnol Rep 4:139–146
Tatke P, Jaiswal Y (2011) An overview of microwave assisted extraction and its applications in herbal drug research. J Med Plant Res 5:21–31

Tian Z, Hwang W, Kim YJ (2019) Mechanistic understanding of monovalent cation transport in eumelanin pigments. J Mater Chem B 7:6355–6361

Van der Heide P (2011) X-ray photoelectron spectroscopy: an introduction to principles and practices. Wiley, New york

Vasanthabharathi V, Lakshminarayanan R, Jayalakshmi S (2011) Melanin production from marine *Streptomyces*. Afr J Biotechnol 10:11224–11234

Wibowo JT, Kellermann MY, Petersen LE, Alfiansah YR, Lattyak C, Schupp PJ (2022) Characterization of an insoluble and soluble form of melanin produced by *Streptomyces cavourensis* SV 21, a sea cucumber associated bacterium. Mar Drugs 20:54

Xiao M, Chen W, Li W, Zhao J, Hong YL, Nishiyama Y, Miyoshi T, Shawkey MD, Dhinojwala A (2018) Elucidation of the hierarchical structure of natural eumelanins. J R Soc Interface 15: 20180045

Yildirim A, Bayindir M (2014) Turn-on fluorescent dopamine sensing based on in situ formation of visible light emitting polydopamine nanoparticles. Anal Chem 86:5508–5512

Youngchim S, Morris-Jones R, Hay RJ, Hamilton AJ (2004) Production of melanin by *Aspergillus fumigatus*. J Med Microbiol 53:175–181

Zdybel M, Pilawa B, Drewnowska JM, Swiecicka I (2017) Comparative EPR studies of free radicals in melanin synthesized by *Bacillus weihenstephanensis* soil strains. Chem Phys Lett 679:185–192

Zhou X, McCallum NC, Hu Z, Cao W, Gnanasekaran K, Feng Y, Stoddart JF, Wang Z, Gianneschi NC (2019) Artificial allomelanin nanoparticles. ACS Nano 13:10980–10990

Zou Y, Xie C, Fan G, Gu Z, Han Y (2010) Optimization of ultrasound-assisted extraction of melanin from *Auricularia auricula* fruit bodies. Innovative Food Sci Emerg Technol 11:611–615